Research Article

Synthesis and Crystal Structure of the Bioinorganic Complex [Sb(Hedta)]·2H$_2$O

Di Li and Guo-Qing Zhong

State Key Laboratory Cultivation Base for Nonmetal Composite and Functional Materials, School of Material Science and Engineering, Southwest University of Science and Technology, Mianyang 621010, China

Correspondence should be addressed to Guo-Qing Zhong; zgq316@163.com

The antimony(III) complex [Sb(Hedta)]·2H$_2$O was synthesized with ethylenediaminetetraacetic acid (H$_4$edta) and antimonous oxide as main raw materials in aqueous solution. The composition and structure of the complex were characterized by elemental analysis, infrared spectra, single crystal X-ray diffraction, X-ray powder diffraction, thermogravimetry, and differential scanning calorimetry. The crystal structure of the antimony(III) complex belongs to orthorhombic system, space group Pna2(1), with cell parameters of a = 18.4823(18) Å, b = 10.9408(12) Å, c = 7.3671(5) Å, V = 1489.7(2) Å^3, Z = 4, and D_c = 1.993 g cm^{-3}. The Sb(III) ion is five-coordinated by two amido N atoms and three carboxyl O atoms from a single Hedta^{3-} ligand, forming a distorted trigonal bipyramid geometry. The thermal decomposition processes of the complex include dehydration, oxidation, and pyrolysis of the ligand, and the last residue is Sb$_2$O$_3$ at the temperature of 570°C.

1. Introduction

Many of the antimony(III) compounds have been mainly used in the clinic medicine because of their medicinal utility and biological activity. The aminopolycarboxylate complexes of antimony(III) with effective antimicrobial and anticancer activity are widely applied to the treatment of a variety of microbial infections including leishmaniasis, diarrhea, peptic ulcers, and helicobacter pylori, and so forth [1, 2]. The ethylenediaminetetraacetic acid as one of the multicarboxylate ligands possesses diverse functional groups such as N-donor and O-donor. When a metal ion is in the center position, the ligand is always allowed to bend and to rotate, and one can easily imagine the structural diversity of new synthesizable materials [3]. In fact, the design and synthesis of metal-organic frameworks (MOFs) is not only because of their fascinating structures and topological novelty, but also because of their existing potential applications as functional materials in gas storage, heterogeneous catalysis, chemical separations, and microelectronics [4–11]. So, the ethylenediaminetetraacetic acid (H$_4$edta) as ligand is a good choice for building a diversified structure; it is not only a plurality

of coordination sites but also an inexpensive and relative safe substance, which can remove toxic heavy metals, reduce oxidative stress, and increase waste excretion [12, 13]. In clinical practice, the chelation therapy with H$_4$edta can prevent cancer and catalytic reactive oxygen species, such as cardiovascular and arteriosclerotic heart disease [14–16]. So, it is widely used in the pharmaceutical and biological aspects.

As we know, the main group elements do not easily form complexes with organic ligands because of the special properties. But, owing to the presence of a lone pair of electrons, showing stereochemical behavior, the antimony complexes with aminopolycarboxylate ligands have attracted people's interests [17]. Because the inorganic salts of antimony(III) have considerable toxicity, so the new biological activity and medicinal function complexes of the main group element antimony are received more attention [18, 19]. Besides, some antimony(III) compounds have been used as antiparasitic agents, and exhibit significant functions as biocides, fungicides, antioxidants, and potential therapeutic agents. For example, some antimony compounds are used for treatment of leishmaniasis, various species of the protozoan leishmania virus and cancer [20–25].

TABLE 1: Crystal data and structure refinement for the title complex.

Empirical formula	$SbC_{10}H_{17}N_2O_{10}$	$F(000)$	888
Formula weight	447.01	Crystal size	$0.46\,mm \times 0.40\,mm \times 0.35\,mm$
Wavelength	0.71073 Å	Theta range for data collection	2.89–25.02°
Temperature	298(2) K	Limiting indices	$-21 \leq h \leq 16, -13 \leq k \leq 13, -7 \leq l \leq 8$
Crystal system	Orthorhombic	Reflections collected/unique	7102/2529 [R(int) = 0.0461]
Space group	Pna2(1)	Completeness to theta = 25.02	99.9%
Unit cell dimensions		Absorption correction	Semiempirical from equivalents
a	18.4823(18) Å	Max. and min. transmission	0.5547 and 0.4738
b	10.9408(12) Å	Refinement method	Full-matrix least-squares on F^2
c	7.3671(5) Å	Date/restraints/parameters	2529/1/208
β	90.00°	Goodness-of-fit on F^2	1.040
V	1489.7(2) Å^3	Final R indices [$I > 2\sigma(I)$]	$R_1 = 0.0332, wR_2 = 0.0811$
Z	4	R indices (all data)	$R_1 = 0.0359, wR_2 = 0.0832$
Calculated density	1.993 g cm^{-3}	Absolute structure parameter	−0.27(4)
Absorption coefficient	1.909 mm^{-1}	Largest diff. peak and hole	0.786 and −0.805 e Å^{-3}

In recent years, owing to the development of aminopoly-carboxylic acid complexes of antimony(III) in medicine, the complex of antimony with multicarboxylate ligands has received more and more attention. Herein, we report the syntheses of the title complex [Sb(Hedta)]·2H$_2$O. The composition and crystal structure of the complex have been characterized by elemental analysis, single crystal X-ray diffraction, XRD, FTIR, and TG-DSC.

2. Experimental

2.1. Materials and General Methods. All the chemicals used in the experiments were analytical reagent as received from commercial sources and without further purification. The ethylenediaminetetraacetic acid and antimonous oxide were purchased from Shanghai Reagent Industry.

The antimony was determined by a Thermo X-II inductively coupled plasma mass spectrometer. The content of carbon, hydrogen, and nitrogen in the complex was measured by a Vario EL CUBE elemental analyzer. The IR spectra were obtained with a Perkin-Elmer Spectrum One-spectrometer in the range of 225–4000 cm^{-1} using KBr pellets. The thermogravimetric analysis of the metal complex was performed by an SDT Q600 thermogravimetric analyzer, and the measurement was recorded from 30 to 800°C at the heating rate of 10°C min^{-1} under air flow of 100 mL min^{-1}. The X-ray powder diffraction was performed using a D/max-II X-ray diffractometer, Cu K$_\alpha$ radiation (λ = 0.154056 nm, step width: 2θ = 0.2°, scan speed: 8°/min).

2.2. Synthesis of the Complex [Sb(Hedta)]·2H$_2$O. The title complex was obtained by aqueous solution synthesis. First, 1.46 g (5 mmol) ethylenediaminetetraacetic acid was solubilized in 200 mL boiling distilled water. Then, 0.875 g (3 mmol) antimonous oxide was gradually added to the above solution, stirring and maintaining the temperature at 90°C. After four hours, when the pH was about 2-3, the reaction was stopped. The unreacted antimonous oxide was filtered. The colorless

filtrate was slowly concentrated to 100 mL. The concentrated solution was placed at room temperature for about one week, and the colorless flaky crystals of the antimony(III) complex was obtained. The yield was about 82%. Anal. Calcd for the title complex, SbC$_{10}$H$_{17}$N$_2$O$_{10}$ (%): Sb, 27.24; C, 26.87; N, 6.27; H, 3.83. Found (%): Sb, 27.11; C, 26.68; N, 6.19; H, 3.74.

2.3. X-Ray Diffraction Crystallography. The appropriate crystals were cut from larger crystals and mounted on a Bruker Smart Apex II CCD diffractometer with graphite monochromated Mo K$_\alpha$ radiation (λ = 0.71073 Å). The data were collected at 298(2) K. A colorless and transparent crystal with dimensions 0.46 mm × 0.40 mm × 0.35 mm was mounted on a glass fiber. Diffraction data were collected in ω mode in the range of 2.89°–25.02°. The structure was solved by direct methods SHELXS-97 and refined by full-matrix least-squares using SHELXL-97 [26, 27]. All nonhydrogen atoms were obtained from the difference Fourier map and full-matrix least-squares refinements on F^2 were carried out with anisotropic thermal parameters. Hydrogen atoms of the ligand were generated geometrically. The structure refinement parameters for the title complex are given in Table 1, and the crystallographic data are deposited with the Cambridge Crystallographic Data Centre under deposition number CCDC 953660.

3. Results and Discussion

3.1. X-Ray Crystal Structure Analysis. The single crystal X-ray diffraction analysis reveals that the complex [Sb(Hedta)]·2H$_2$O crystallises in the orthorhombic system with space group Pna2(1). Crystallographic data and structure refinement parameters for the title complex are given in Table 1, and the selected bond distances and angles are shown in Table 2. The key fragments of the structures and the atom numbering are shown in Figure 1, and the crystal packing diagram of the complex is shown in Figure 2. The asymmetric unit of the complex consists of one Hedta^{3-}, one trivalent antimony

TABLE 2: Selected bond lengths (Å) and angles (°) for the title complex.

Sb(1)–O(1)	2.182(4)	O(7)–C(9)	1.218(7)	N(1)–Sb(1)–N(2)	75.9(2)
Sb(1)–O(5)	2.199(4)	O(8)–C(9)	1.299(7)	C(4)–N(1)–Sb(1)	107.5(3)
Sb(1)–O(3)	2.243(4)	O(1)–Sb(1)–O(5)	142.8(2)	C(6)–N(1)–Sb(1)	108.6(4)
Sb(1)–N(1)	2.336(5)	O(1)–Sb(1)–O(3)	104.36(16)	C(1)–N(1)–Sb(1)	109.7(3)
Sb(1)–N(2)	2.402(5)	O(5)–Sb(1)–O(3)	85.38(15)	C(8)–N(2)–Sb(1)	104.8(3)
O(1)–C(3)	1.307(8)	O(1)–Sb(1)–N(1)	74.09(16)	C(2)–N(2)–Sb(1)	108.5(3)
O(2)–C(3)	1.222(7)	O(5)–Sb(1)–N(1)	75.60(18)	C(10)–N(2)–Sb(1)	114.9(4)
O(3)–C(5)	1.273(7)	O(3)–Sb(1)–N(1)	71.03(17)	C(3)–O(1)–Sb(1)	120.0(4)
O(4)–C(5)	1.229(7)	O(1)–Sb(1)–N(2)	78.88(16)	C(7)–O(5)–Sb(1)	118.9(4)
O(5)–C(7)	1.286(7)	O(5)–Sb(1)–N(2)	73.26(17)	C(5)–O(3)–Sb(1)	120.1(4)
O(6)–C(7)	1.238(7)	O(3)–Sb(1)–N(2)	144.17(16)		

TABLE 3: Hydrogen bond lengths (Å) and bond angles (°) for the title complex.

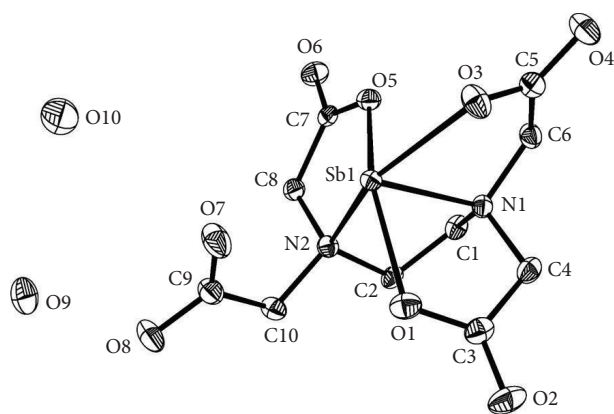| D–H	d(D–H)	d(H···A)	d(D···A)	∠DHA	A symmetry operation
O8–H8	0.820	1.742	2.556	171.90	O9
O9–H9C	0.850	1.854	2.702	175.29	O4 $\left[-x+\frac{1}{2}, y+\frac{1}{2}, z+\frac{1}{2}\right]$
O9–H9D	0.850	1.935	2.783	175.28	O6 $\left[-x+1, -y+1, z+\frac{1}{2}\right]$
O10–H10E	0.850	2.110	2.950	169.24	O9
O10–H10F	0.850	2.091	2.930	169.18	O2 $\left[-x+\frac{1}{2}, y-\frac{1}{2}, z+\frac{1}{2}\right]$

FIGURE 1: The molecular structure of the title complex.

ion, and two crystalline water molecules. Sb(III) ion for plane forms a distorted trigonal bipyramidal configuration. The Sb(III) ion is five-coordinated by three carboxyl oxygen atoms (O1, O3, and O5) and two nitrogen atoms (N1 and N2) from the same Hedta^{3-} ligand. Therefore, a carboxyl group (O7 and O8) and all water molecules in the title complex are not coordinated. The bond lengths of Sb1–O1, Sb1–O3, and Sb1–O5 are in the range of 2.182–2.243 Å, and it belongs to the typical distance of the aminopolycarboxylate complexes of antimony(III) [28]. But, with respect to the bond lengths of C–O, there are two types of carboxyl groups in the complex. The C5(7)–O3(5) is longer than C5(7)–O4(6), about 0.04 Å, like the usual ionized carboxyl group. But, the C3(9)–O1(8) is

longer than C3(9)–O2(7), about 0.08 Å, which is comparable with the value of a free carboxylic acid, and this type of coordination seems to cause the especially strong acidity of Sb-(Hedta). The bond angles of N1–Sb1–O3, N1–Sb1–O5, N1–Sb1–N2, and N1–Sb1–O1 are almost similar; if the Sb1–N1 is perpendicular to the equator plane, they look like an inverted umbrella, and the Sb–N bond lengths are 2.336(5) Å and 2.402(5) Å, and the Sb–O band lengths are Sb1–O1 = 2.182(4) Å, Sb1–O3 = 2.243(4) Å, and Sb1–O5 = 2.199(4) Å, respectively.

In Tables 2 and 3, there are three types of hydrogen bonds in the crystal of the Sb(III) complex, and they include the weak hydrogen bonds between the crystalline water molecules (O10–H10E···O9, 2.950 Å), the crystalline water and the oxygen atoms of the carbonyl groups (O9–H9C···O4, 2.702 Å; O9–H9D···O6, 2.783 Å, and O10–H10F···O2, 2.930 Å), and the strong hydrogen bonds between the crystalline water and the oxygen atoms of the hydroxyl groups (O8–H8···O9, 2.556 Å). In Figure 3, because there are a lot of crystal water molecules in the complex, the interstitial water molecules and the carboxyl oxygen atoms will form hydrogen bonds, which make the structure more stable.

3.2. X-Ray Powder Diffraction. The X-ray powder diffraction data of [Sb(Hedta)]·2H$_2$O was collected in the diffraction angle range of 3°–80°. The XRD pattern of the complex is shown in Figure 4(a). The main diffraction peaks appear at $2\theta = 9.56°, 15.30°$, and $16.85°$ for the title complex. The index calculation of the XRD data bases on the computer program of least squares method [29] and the calculated results are
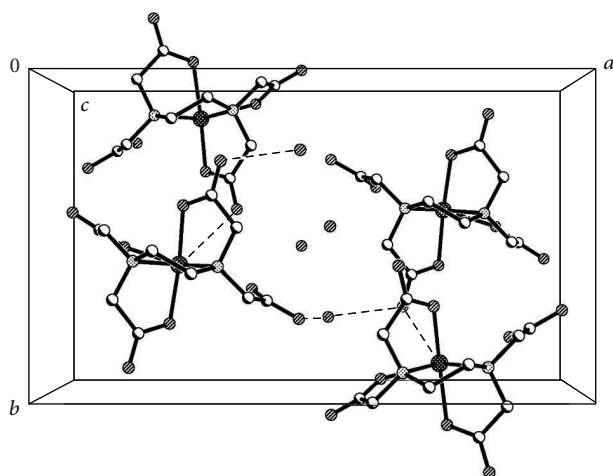
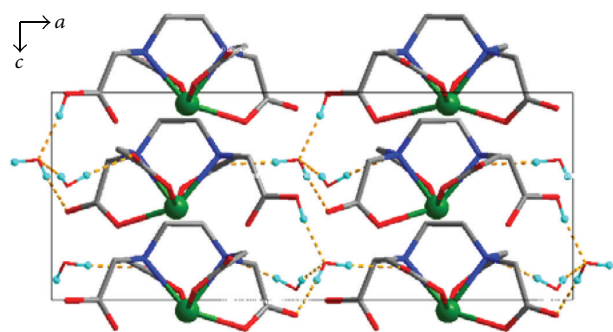FIGURE 2: Crystal packing diagram of the title complex.

FIGURE 3: Packing diagram of the title complex showing H bonding along the b axis.
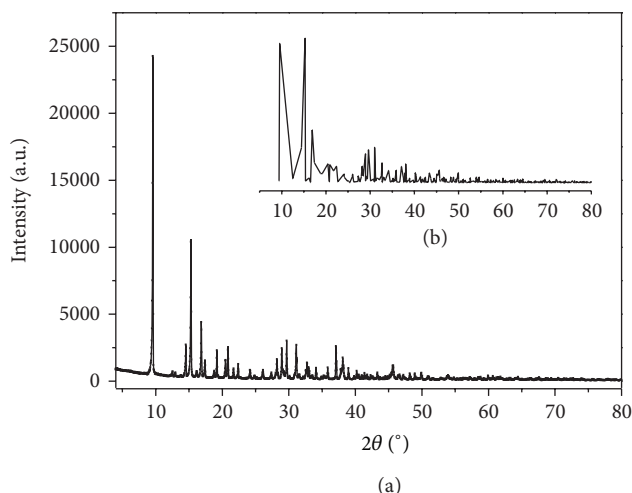

(a)

FIGURE 4: XRD patterns for title complex generated from the experimental data (a) and simulated from the single crystal X-ray data (b).
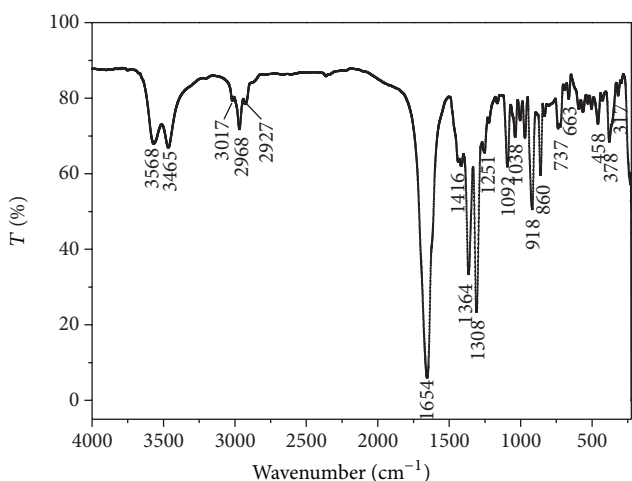

FIGURE 5: FT-IR spectra of the title complex.

shown in Table 4. Table 4 shows that the calculated spacing d_{hkl} is consistent with the experimental ones, and the largest relative deviation between the experimental and calculated spacing d_{hkl} is less than 0.3%. This indicates that the resultant is a single phase compound [17]. The crystal structure of the complex belongs to an orthorhombic system with the lattice parameters: $a = 18.479$ Å, $b = 10.957$ Å, and $c = 7.343$ Å, respectively. The results of indexes to the XRD data for the complex are consistent with the results of single crystal. The experimental pattern exhibiting some peaks is slightly broadened in comparison with the simulated pattern in Figure 4(b), which may be due to the preferred orientation of the powder samples. The experimental XRD pattern agrees well with the simulated pattern generated on the basis of the single crystal analyses for the title complex.

3.3. FT-IR Spectra. The FT-IR spectra of the title complex are shown in Figure 5. The infrared spectra of the complex show that wide absorption bands in the region 3400–3600 cm^{-1} can be assigned to the O–H stretching vibration of the water molecules. The peaks observed from 3017 to 2927 cm^{-1} are in good agreement with the C–H vibrations. If the band at 1700–1750 cm^{-1} shows the existence of a free carboxyl group, while at about 1650 cm^{-1}, suggests that carboxyl groups are

coordinated. In which, the ν_{as}(COO) band of the complex [Sb(Hedta)]·2H$_2$O appears at 1654 cm^{-1}, both 1364 cm^{-1} and 1308 cm^{-1} are the ν_s(COO) bands The difference value of 290 cm^{-1} and 346 cm^{-1} between the asymmetric and symmetric stretching vibration of the carboxylate group is in line with a monodentate type of coordination [29]. In addition, 1092 cm^{-1} is the specific absorption peak about the C–N vibrations. Compared with the Na$_2$H$_2$edta ligand, the C–N at 1137 cm^{-1} shifts towards lower frequencies, and it confirms that the nitrogen atoms of the ligand are coordinated to the Sb(III) ion. In the far-infrared region, the absorption peak found in the 378 cm^{-1} region is assigned to the ν(Sb–N) vibration and in the 317 cm^{-1} region is assigned to the ν(Sb–O) stretching vibration.

3.4. Thermal Analysis. The thermal decomposition process of complexes can help us understand the coordination structure

TABLE 4: Experimental data and calculated results for powder X-ray diffraction pattern of the complex [Sb(Hedta)]·2H$_2$O (orthorhombic system: a = 18.479 Å, b = 10.957 Å, and c = 7.343 Å).

No.	2θ (°)	h	k	l	$d_{\exp}$ (Å)	d_{cal} (Å)	I/I_0
1	9.56	2	0	0	9.242	9.240	100.0
2	12.52	2	1	0	7.064	7.063	1.5
3	12.96	1	0	1	6.827	6.824	1.2
4	14.51	0	1	1	6.100	6.100	9.5
5	15.30	1	1	1	5.788	5.792	42.6
6	16.17	0	2	0	5.477	5.478	1.6
7	16.85	1	2	0	5.256	5.253	17.2
8	17.41	2	1	1	5.090	5.091	5.2
9	18.11	2	2	0	4.713	4.712	2.1
10	19.19	4	0	0	4.621	4.620	8.5
11	20.48	3	1	1	4.332	4.334	5.5
12	20.85	4	1	0	4.257	4.257	9.7
13	21.69	3	2	0	4.094	4.094	3.0
14	22.40	2	2	1	3.966	3.966	4.5
15	24.15	4	1	1	3.682	3.683	2.7
16	24.86	1	3	0	3.579	3.583	0.9
17	26.10	2	0	2	3.411	3.412	2.8
18	27.37	2	1	2	3.256	3.258	1.8
19	28.21	3	0	2	3.160	3.154	5.9
20	28.95	6	0	0	3.081	3.080	9.4
21	29.69	1	2	2	3.007	3.009	11.8
22	31.12	4	0	2	2.871	2.874	10.6
23	31.61	5	2	1	2.828	2.828	1.3
24	32.73	3	2	2	2.733	2.733	5.0
25	33.00	1	4	0	2.712	2.710	3.6
26	33.54	4	3	1	2.670	2.669	1.1
27	34.10	2	4	0	2.627	2.626	3.4
28	35.24	1	4	1	2.544	2.542	1.1
29	35.84	3	4	0	2.503	2.503	3.5
30	37.07	1	0	3	2.423	2.426	10.2
31	37.80	7	2	0	2.378	2.378	3.0
32	38.11	2	0	3	2.360	2.366	6.7
33	38.95	2	1	3	2.311	2.313	3.4
34	39.81	4	3	2	2.262	2.259	0.8
35	40.18	4	4	1	2.242	2.244	2.5
36	40.50	1	2	3	2.225	2.219	1.2
37	40.95	0	4	2	2.202	2.196	0.9
38	41.39	2	2	3	2.178	2.172	1.7
39	41.77	4	0	3	2.161	2.163	1.2
40	42.28	7	0	2	2.137	2.143	1.1
41	43.31	1	5	1	2.087	2.086	1.9
42	45.19	4	2	3	2.006	2.012	1.3
43	45.69	2	3	3	1.984	1.986	4.1
44	46.62	8	3	0	1.947	1.952	1.3
45	47.18	3	3	3	1.926	1.931	1.2
46	48.17	5	4	2	1.888	1.888	1.8
47	48.93	4	3	3	1.860	1.861	1.8

TABLE 4: Continued.

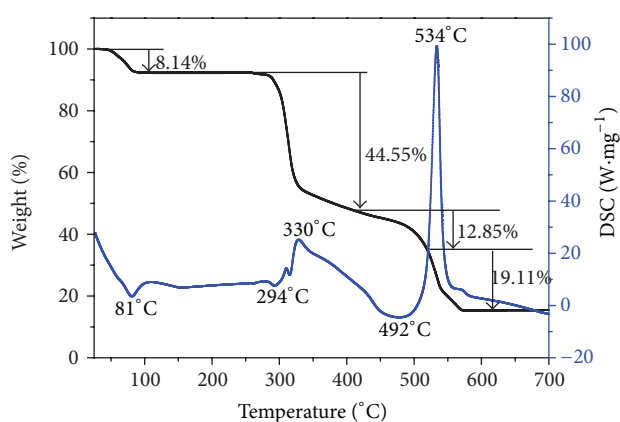| No.	2θ (°)	h	k	l	$d_{\exp}$ (Å)	d_{cal} (Å)	I/I_0
48	49.89	0	4	3	1.826	1.825	1.9
49	50.90	2	4	3	1.792	1.791	1.0
50	53.92	4	4	3	1.698	1.697	1.3
51	58.45	3	6	2	1.578	1.580	0.8
52	58.77	0	7	0	1.569	1.565	0.8
53	59.94	2	7	0	1.542	1.543	1.2
54	60.66	0	4	4	1.525	1.525	1.1
55	61.79	5	3	4	1.500	1.499	0.9
56	64.46	2	1	5	1.442	1.438	0.9
57	67.57	2	5	4	1.388	1.391	0.9

FIGURE 6: TG-DSC curves of the title complex.

of the complexes [30]. The TG-DSC curves of the title complex are given in Figure 6, and the possible pyrolysis reaction and the experimental and calculated percentage mass losses in the thermal decomposition process of the complex are summarized in Table 5. The first mass loss of the complex [Sb(Hedta)]·2H$_2$O occurs about 81°C in DSC curve, corresponding to the release of two molecules in crystalline water. This is consistent with the single crystal structure. The experimental percentage mass loss (8.14%) is close to the calculated one (8.06%). Then, a small endothermic peak in DSC curve appears at 294°C. Because there is not any corresponding mass loss of the sample in the TG curve, it can be attributable to structure rearrangement or phase transformation in the solid complex. Thereafter, the exothermic peak at 330°C corresponds to oxidation and decomposition of the ligand, and the experimental mass loss (44.55%) is close to the calculated one (44.57%). This step decomposition product is Sb$_2$(CO$_3$)$_3$. Then, Sb$_2$(CO$_3$)$_3$ is decomposed into Sb$_2$O$_4$ (Scheme 1), and the experimental and theoretical mass losses are 12.85% and 12.98%, respectively. This is why there is an appreciable endothermic peak at 492°C in DSC curve. However, some of the compounds of antimony may be volatile at high temperature. The final step of the exothermic peak appears at 534°C in DSC curve. The Sb–O single bond is ruptured, and then half of the antimony compound may

TABLE 5: Thermal decomposition data of the title complex.

Reaction	DSC (°C)	Mass loss (%)	
		W_{exp}	W_{theor}
$[Sb(Hedta)]\cdot 2H_2O$			
$\downarrow -2H_2O$	81 (endo.)	8.14	8.06
$[Sb(Hedta)]$			
$\downarrow$ structural rearrangement	294 (endo.)		
$[Sb(Hedta)]$			
$\downarrow -C_{8.5}H_{13}N_2O_{3.5}$	330 (exo.)	44.55	44.57
$1/2Sb_2(CO_3)_3$			
$\downarrow -C_3O_5$	492 (exo.)	12.85	12.98
$1/2Sb_2O_4$			
$\downarrow -Sb_{0.5}O_{1.25}$	534 (endo.)	19.11	18.09
$1/4Sb_2O_3$		15.35[a]	16.30[b]

[a]The experimental percentage mass of the residue in the sample; [b]the calculated percentage mass of the residue in the sample.
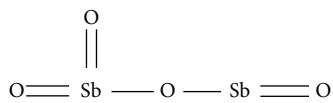
SCHEME 1: Structure of the Sb_2O_4.

be oxidized and volatilized. The final residue is antimonous oxide, and the experimental result (15.35%) is in agreement with the result of theoretical calculation (16.30%).

4. Conclusion

The complex $[Sb(Hedta)]\cdot 2H_2O$ was synthesized with the reaction of ethylenediaminetetraacetic acid and antimonous oxide as the reactants. The composition and structure of the complex were characterized by EA, singlerystal X-ray diffraction, XRD, FTIR, and TG-DSC. The crystal structure of the complex belongs to orthorhombic system, space group Pna2(1), with cell parameters of $a = 18.4823(18)$ Å, $b = 10.9408(12)$ Å, $c = 7.3671(5)$ Å, $Z = 4$, and $D_c = 1.993$ g cm^{-3}. Sb(III) ion is five-coordinated by two amido N atoms and three carboxyl O atoms from a single Hedta^{3-} ligand, forming a distorted trigonal bipyramid geometry.

5. Extra Material

Crystallographic data for the title complex $[Sb(Hedta)]\cdot 2H_2O$ has been deposited with the Cambridge Crystallographic Data Centre. The deposition number is CCDC-953660. The data can be obtained free of charge on application to the Director, CCDC, 12 Union Road, Cambridge, CB2 1EZ, UK, fax: +44 1223 366 033, e-mail: deposit@ccdc.ac.uk, or on the web: www: http://www.ccdc.cam.ac.uk, or from the authors up on request.

Conflict of Interests

The authors declare that there is no conflict of interests regarding the publication of this paper.

Acknowledgments

References

[1] J. A. Lessa, D. C. Reis, I. C. Mendes et al., "Antimony(III) complexes with pyridine-derived thiosemicarbazones: structural studies and investigation on the antitrypanosomal activity," *Polyhedron*, vol. 30, no. 2, pp. 372–380, 2011.

[2] D. C. Reis, M. C. X. Pinto, E. M. Souza-Fagundes, S. M. S. V. Wardell, J. L. Wardell, and H. Beraldo, "Antimony(III) complexes with 2-benzoylpyridine-derived thiosemicarbazones: cytotoxicity against human leukemia cell lines," *European Journal of Medicinal Chemistry*, vol. 45, no. 9, pp. 3904–3910, 2010.

[3] A. Y. Robin and K. M. Fromm, "Coordination polymer networks with O- and N-donors: what they are, why and how they are made," *Coordination Chemistry Reviews*, vol. 250, no. 15-16, pp. 2127–2157, 2006.

[4] J. Cui, Y. Li, Z. Guo, and H. Zheng, "A porous metal-organic framework based on Zn_6O_2 clusters: chemical stability, gas adsorption properties and solvatochromic behavior," *Chemical Communications*, vol. 49, no. 6, pp. 555–557, 2013.

[5] G. H. Cui, C. H. He, C. H. Jiao, J. C. Geng, and V. A. Blatov, "Two metal-organic frameworks with unique high-connected binodal network topologies: synthesis, structures, and catalytic properties," *Chemical Engineering Communications*, vol. 14, no. 12, pp. 4210–4216, 2012.

[6] X. L. Zhao, D. Sun, S. Yuan et al., "Comparison of the effect of functional groups on gas-uptake capacities by fixing the volumes of cages A and B and modifying the inner wall of cage C in rht-type MOFs," *Inorganic Chemistry*, vol. 51, no. 19, pp. 10350–10355, 2012.

[7] S. R. Kim, K. W. Dawson, B. S. Gelfand, J. M. Taylor, and G. K. Shimizu, "Enhancing proton conduction in a metal-organic framework by isomorphous ligand replacement," *Journal of the American Chemical Society*, vol. 135, no. 3, pp. 963–966, 2013.

[8] X. T. Zhang, D. Sun, B. Li, L. M. Fan, B. Li, and P. H. Wei, "Unusual high thermal stablility of a 2D → 3D polycatenated Fe(II) metal-organic framework showing guest-dependent spin-crossover behavior and high spin-transition temperature," *Crystal Growth & Design*, vol. 12, no. 8, pp. 3845–3848, 2012.

[9] J.-P. Zhang, Y.-B. Zhang, J.-B. Lin, and X.-M. Chen, "Metal azolate frameworks: from crystal engineering to functional materials," *Chemical Reviews*, vol. 112, no. 2, pp. 1001–1033, 2012.

[10] D. Sun, G.-G. Luo, N. Zhang, R.-B. Huang, and L.-S. Zheng, "Simultaneous self-assembly of a cage-like silver(i) complex encapsulating an Ag6 neutral cluster core and carbon dioxide fixation," *Chemical Communications*, vol. 47, no. 5, pp. 1461–1463, 2011.

[11] D. Banerjee and J. B. Parise, "Recent advances in s-block metal carboxylate networks," *Crystal Growth and Design*, vol. 11, no. 10, pp. 4704–4720, 2011.

[12] K. C. Atwood IV, E. Woockner, R. S. Baratz, and W. I. Sampson, "Why the NIH Trial to Assess Chelation Therapy (TACT) should be abandoned," *MedGenMed Medscape General Medicine*, vol. 10, no. 5, article 115, 2008.

[13] W. Blumer and E. M. Cranton, "Ninety percent reduction in cancer mortality after chelation therapy with EDTA," *Journal of Advancement in Medicine*, vol. 2, no. 1-2, pp. 183–188, 1989.

[14] A. M. van Rij, C. Solomon, S. G. K. Packer, and W. G. Hopkins, "Chelation therapy for intermittent claudication: a double-blind, randomized, controlled trial," *Circulation*, vol. 90, no. 3, pp. 1194–1199, 1994.

[15] E. Ernst, "Chelation therapy for coronary heart disease: an overview of all clinical investigations," *American Heart Journal*, vol. 140, no. 1, pp. 139–141, 2000.

[16] M. L. Knudtson, D. G. Wyse, P. D. Galbraith et al., "Chelation therapy for ischemic heart disease: a randomized controlled trial," *Journal of the American Medical Association*, vol. 287, no. 4, pp. 481–486, 2002.

[17] G. Q. Zhong and Y. C. Guo, "Studies on synthesis and indexes of X-ray powder diffraction data of hydrogen ethylenediamine terraacetato-antimony(III) monohydrate," *Journal of Changde Teachers University*, vol. 14, no. 3, pp. 39–42, 2002.

[18] A.-K. Leuz, H. Mönch, and C. A. Johnson, "Sorption of Sb(III) and Sb(V) to goethite: influence on Sb(III) oxidation and mobilization," *Environmental Science and Technology*, vol. 40, no. 23, pp. 7277–7282, 2006.

[19] M. Filella, N. Belzile, and Y.-W. Chen, "Antimony in the environment: a review focused on natural waters II. Relevant solution chemistry," *Earth-Science Reviews*, vol. 59, no. 1–4, pp. 265–285, 2002.

[20] S. Rais, A. Perianin, M. Lenoir et al., "Sodium stibogluconate (Pentostam) potentiates oxidant production in murine visceral leishmaniasis and in human blood," *Antimicrobial Agents and Chemotherapy*, vol. 44, no. 9, pp. 2406–2410, 2000.

[21] R. C. Palenik, K. A. Abboud, and G. J. Palenik, "Bond valence sums and structural studies of antimony complexes containing Sb bonded only to O ligands," *Inorganica Chimica Acta*, vol. 358, no. 4, pp. 1034–1040, 2005.

[22] G. Cantos, C. L. Barbieri, M. Iacomini, P. A. J. Gorin, and L. R. Travassos, "Synthesis of antimony complexes of yeast mannan and mannan derivatives and their effect on Leishmania-infected macrophages," *Biochemical Journal*, vol. 289, no. 1, pp. 155–160, 1993.

[23] J. Shen, B. Jin, Q. Jiang, G. Zhong, Y. Hu, and J. Huo, "Synthesis, characterization, and magnetic properties of heterometallic trinuclear complex with Sb(III) and Ho(III)," *Inorganica Chimica Acta*, vol. 385, pp. 158–163, 2012.

[24] P. Sharma, D. Perez, A. Cabrera, N. Rosas, and J. L. Arias, "Perspectives of antimony compounds in oncology," *Acta Pharmacologica Sinica*, vol. 29, no. 8, pp. 881–890, 2008.

[25] S. K. Hadjikakou, C. D. Antoniadis, N. Hadjiliadis et al., "Synthesis and characterization of new water stable antimony(III) complex with pyrimidine-2-thione and in vitro biological study," *Inorganica Chimica Acta*, vol. 358, no. 10, pp. 2861–2866, 2005.

[26] G. M. Sheldrick, *SHELXS 97, Program for the Solution of Crystal Structure*, University of Göttingen, 1997.

[27] G. M. Sheldrick, *SHELXS 97, Program for the Refinement of Crystal Structure*, University of Göttingen, 1997.

[28] M. Shimoi, Y. Orita, T. Uehiro et al., "The Structure of (hydrogen ethylenediaminetetraacetato) antimony(III) dihydrate $Sb(C_{10}H_{13}N_2O_8) \cdot 2H_2O$," *Bulletin of the Chemical Society of Japan*, vol. 53, no. 11, pp. 3189–3194, 1980.

[29] G.-Q. Zhong, Y.-C. Guo, Y.-R. Chen, X.-S. Zang, and S.-R. Luan, "Synthesis and crystal structure of the complex of thioglycollic acid and trivalent antimony ion," *Acta Chimica Sinica*, vol. 59, no. 10, pp. 1599–1603, 2001.

[30] G. Q. Zhong, J. Shen, Q. Y. Jiang, Y. Q. Jia, M. J. Chen, and Z. P. Zhang, "Synthesis, characterization and thermal decompositionof Sb^{III}-M-Sb^{III} type trinuclear complexes of ethylenediamine-N, N, N', N'-tetraacetate (*M*:Co(II), La(III), Nd(III), Dy(III))," *Journal of Thermal Analysis and Calorimetry*, vol. 92, no. 2, pp. 607–616, 2008.